

1 **Experimental study of a sustainable cooling process hybridizing indirect evaporative cooling and**
2 **mechanical vapor compression**

3
4 Qian Chen^{1,*}, M Kum Ja¹, Muhammad Burhan¹, Muhammad Wakil Shahzad^{1,2}, Doskhan Ybyraiymkul¹, Ho
5 ngfei Zheng³, Kim Choon Ng^{1,*}

- 6 1. *Water Desalination and Reuse Center, Biological and Environmental Science and Engineering Divi*
7 *sion, King Abdullah University of Science and Technology, Thuwal 23955, Saudi Arabia*
8 2. *Northumbria University, Newcastle upon Tyne, United Kingdom*
9 3. *School of Mechanical Engineering, Beijing Institute of Technology, Beijing 100081, China*

10
11 *Corresponding authors, email: chen_qian@u.nus.edu; kimchoon.ng@kaust.edu.sa

12
13 **Abstract**

14 The hybrid indirect evaporative cooling-mechanical vapor compression (IEC-MVC) process is an emerging
15 cooling technology that combines the advantages of IEC and MVC, i.e., effective temperature and humidity
16 control, high energy efficiency, and low water consumption. This paper presents an experimental study of
17 the hybrid IEC-MVC process. A 1-Rton pilot is fabricated by connecting IEC and MVC in series, and its
18 performance is evaluated under different operating conditions (outdoor air temperature and humidity, air
19 flowrate, compressor frequency). Results revealed that the outdoor air temperature and humidity could be
20 lowered to 5-15 °C and 5-10 g/kg, respectively. The IEC handles 35-50% of the total cooling load, and the
21 energy consumption can be reduced by 15-35% as compared to standalone MVC. Moreover, the condensate
22 collected from the evaporator can compensate for >70% of water consumption in IEC, making the system
23 applicable in arid regions. Based on the derived results, a simplified empirical model is developed for rapid
24 evaluation of the IEC-MVC process, and the energy-saving potential in major cities of Saudi Arabia is
25 estimated.

26 *Keywords:* indirective evaporative cooling; mechanical vapor compression; hybrid cooling system;
27 experimental study; rapid evaluation model;

28
29 **1. Introduction**

30 With the growth of the global population and increase of living standards, the demand for air-conditioning
31 (AC) has been increasing rapidly in the past few decades. It is projected that the global AC stock will reach
32 5000 million units by 2050, and the corresponding electricity consumption will exceed 6000 TWh [1].
33 Therefore, reducing the energy consumption for AC is one of the most critical ways to alleviate global
34 energy stress and cut CO₂ emissions.

35 The Gulf Cooperation Council (GCC) region is among the areas that have the highest cooling demands.
36 The annual cooling load in GCC countries exceeds 36 million Rton [2], and the energy consumption of
37 AC accounts for 50-70% of peak electricity demand [2]. The required cooling is mainly provided by
38 mechanical vapor compression (MVC) chillers due to their high technical maturity and low costs. However,
39 MVC suffers from a low energy efficiency in this region due to the high ambient temperature and poor air
40 quality [3, 4]. In order to reduce the primary energy consumption, the industry has been searching for more
41 sustainable alternatives to MVC chillers.

1 The indirect evaporative cooler (IEC) is deemed a promising technology for cooling applications. It utilizes
2 the evaporation of water as the driving force for cooling. As the evaporation heat of water (>2200 kJ/kg) is
3 much higher than the heat capacity of air (~ 1 kJ/kg-°C), substantial cooling effects can be produced by
4 evaporating a small amount of water. The only power input in this process is the electricity consumption of
5 the fans and the water pumps, which is insignificant compared to the cooling power. As a result, the energy
6 efficiency of IEC is several times higher than MVC [5].

7 Extensive research efforts have been reported to improve IEC's performance, and the latest ones can be
8 categorized into the following: (i) proposing novel configurations for IEC heat and mass exchanger, (ii)
9 enhancing heat and mass transfer in dry and wet channels, and (iii) exploring new materials for system
10 fabrication. Conventional IECs are flat-plate heat exchangers with cross-flow or counter-flow
11 configurations [6, 7]. The Maisotsenko-cycle (M-cycle) cooler [8, 9] and the regenerative indirect
12 evaporative cooler (RIEC) [10, 11] are two prominent examples, which can cool the air to below its wet-
13 bulb temperature. Compared with cross-flow, the counter-flow configuration is more complex but
14 demonstrates better performance. For an optimal trade-off between complexity and cooling performance,
15 the counter-cross-flow configuration was recently proposed [12, 13]. Its fabrication is simple like cross-
16 flow IEC, while the cooling performance is close to that of counter-flow IEC. Other novel configurations
17 include the tubular IEC and the heat-pipe IEC. The former has a more uniform water distribution [14, 15],
18 and the latter enhances heat and mass transfer between dry and wet channels [16, 17].

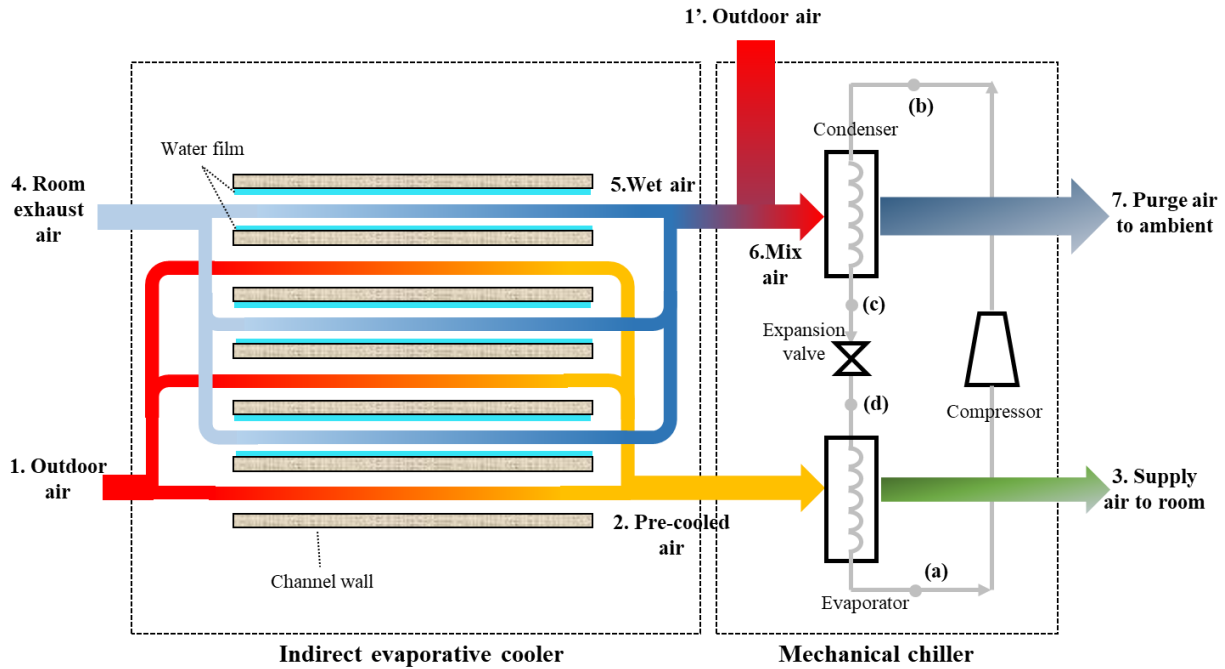
19 Research efforts have also been reported to enhance heat and mass transfer inside IEC by adding internal
20 structures, e.g., corrugated wick structures, baffles, and fins. Corrugated wick structures made from cotton
21 or paper can not only increase the heat and mass transfer area but also improve wettability [18]. Moshari
22 [19] added wick materials in the wet channels of IEC and observed better evaporative cooling effects, but
23 the pressure drop of air was also higher. Kabeel et al. [20, 21] introduced baffles in the dry channels, which
24 created internal vortexes and increased the wet-bulb effectiveness by >33%. Ali et al. [22] added aluminum
25 fins in the dry channels and enhanced the cooling capacity by 18%.

26 The effects of material selection on IEC have also been explored. Aluminum is the most widely used
27 material because of its good thermal conductivity and hydrophilicity [7]. Moreover, the aluminum plate is
28 thin and has negligible thermal resistance [23]. Porous ceramics are another promising option due to their
29 high porosity, good thermal conductivity, and high corrosion resistance [24]. Wang et al. [14] demonstrated
30 that the tubular ceramic IEC could maintain the cooling capacity for 100 min after 5 minutes of water spray.
31 Boukhanouf et al. [25] presented a plate-type IEC made of a ceramic water container. The maximum
32 cooling capacity was 225 W/m², and the wet-bulb effectiveness reached 102.4%. Lee et al. [26] added
33 porous coating on the wet channels of a RIEC and achieved wet-bulb effectiveness of 120%.

34 Despite the above-mentioned efforts, the broader application of IEC is still hindered by several intrinsic
35 limitations. Firstly, the supply air temperature is restricted by the dew-point of the outdoor air, and the
36 desired temperature can't be reached when outdoor air is hot and humid [27]. Secondly, IEC can only
37 handle the sensible load and has little dehumidification capability. Thirdly, IEC consumes water as the
38 driving force of cooling. Due to these limitations, IEC is not suitable for the GCC region, which has severe
39 water scarcity and high ambient humidity.

40 To overcome the intrinsic limitations of IEC, several authors have proposed the hybridization of IEC and
41 MVC [28]. As shown in Figure 1, the IEC and MVC are connected in tandem. The outdoor air is firstly
42 pre-cooled in the IEC and then further processed in the MVC to achieve the desired temperature and
43 humidity. Such a hybrid configuration can effectively control air temperature and humidity while sustaining
44 a high energy efficiency. Moreover, the room return air can be used in the wet channels of IEC to recover
45 the cold energy. Another advantage is that the condensate from the evaporator of MVC can be recovered

1 to replenish the water consumption in IEC. With these promising features, IEC-MVC is suitable for cooling
2 applications in most areas.



3
4 Figure 1 Schematic of the hybrid IEC-MVC process [28]

5
6 The hybrid IEC-MVC process has attracted substantial research interests. Cui et al. [10, 29] studied the
7 potential of the hybrid system in Singapore and found that IEC could handle 32% of the cooling load. Duan
8 et al. [30] studied the performance of IEC-MVC under the climatic conditions of Beijing and observed
9 seasonal energy-saving of 38.2%. Chen et al. [31] evaluated the potential of IEC-MVC in Hong Kong. The
10 payback period was 2.9 years, and the cost-saving was 45% more than the enthalpy recovery wheel. Cui et
11 al. [32] reported similar efforts for five cities: Xi'an, Athinai, Firenze, Cairo, and Singapore, and more than
12 35% of energy-saving potential was observed. Chen et al. [33, 34] developed an analytical model to evaluate
13 the use of IEC as a pre-cooler of MVC. For similar purposes, Pandelidis et al. [35] presented an ϵ -NTU-
14 model, and Min et al. [36] developed a statistical model.

15 In our previous work [28], we presented a preliminary study on the hybrid IEC-MVC process. The IEC was
16 operated as an enthalpy-recovery device to recover cold energy from the room exhaust air, and the
17 effectiveness of enthalpy recovery was empirically correlated to the operating parameters. However, the
18 energy-saving of the hybrid process was estimated analytically without experimental demonstration.
19 Moreover, the previous study only focused on energy efficiency, and the water footprint has not been
20 evaluated.

21 The current study is an extension of our previous work on the IEC-MVC process. A pilot IEC-MVC unit is
22 fabricated and tested under different operating conditions (outdoor air temperature and humidity, air
23 flowrate, compressor frequency), and the system is evaluated in terms of cooling performance, energy
24 efficiency, and water consumption. Based on the experimental results, a simplified model is developed for
25 rapid evaluation of the IEC-MVC process, and a case study is conducted under the climatic conditions of
26 Saudi Arabia.

1
2
3
4
5
6
7
8
9
10
11
12
13
14
15
16
17
18
19
20
21
22
23
24
25

2. Methodology

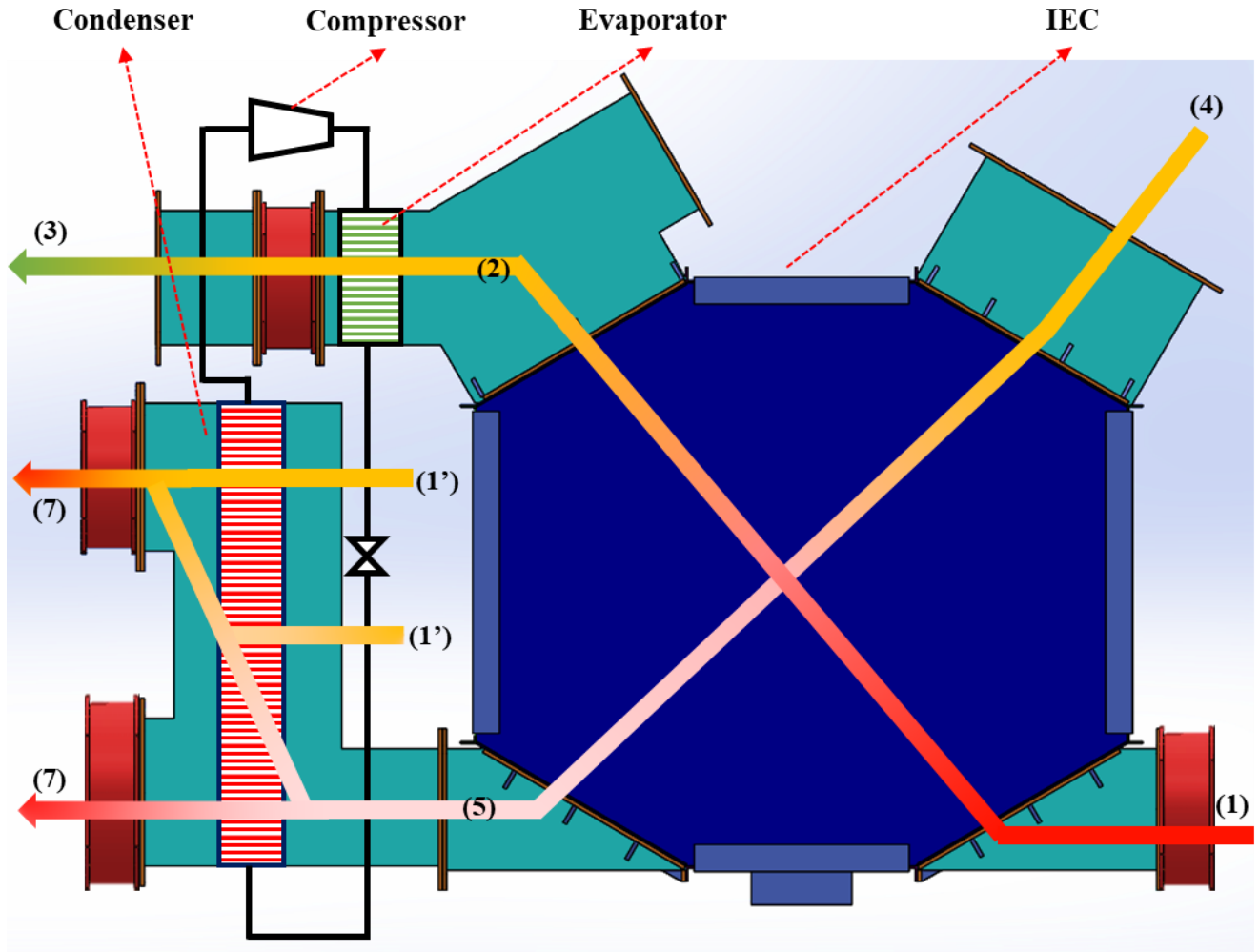
A pilot IEC-MVC unit is commissioned by connecting the IEC unit presented in [28] with an MVC cycle. Sensors are arranged at different locations to monitor the flowrate, temperature, and humidity of the air streams to monitor the system performance. Based on the measured parameters, the cooling performance, energy efficiency and water consumption of the hybrid system are evaluated.

2.1 Experimental design

The pilot IEC unit presented in our previous study [28] is connected with an MVC cycle to form the IEC-MVC process. The IEC consists of 100 dry and wet channels that are arranged in an alternating manner. The channels are separated by aluminum sheets with a thickness of 300 μm . Spray nozzles are installed at the entrance of the wet channels to supply water. Detailed information on the IEC is available in [28].

The MVC unit consists of a compressor, an evaporator, a condenser, and a throttling valve. A commercial scroll compressor (Copeland™ ZR36K3E-TF5-522, Emerson) is selected, and its speed is regulated by a variable frequency drive (Altivar 320, Schneider). R134a is used as the refrigerant due to its broad applications. The evaporator and the condenser are fin-tube heat exchangers made of copper, and they are sized according to the design capacity.

The schematic of the hybrid IEC-MVC unit is shown in Figure 2. The evaporator is placed after the exit of the dry channels, while the condenser is located after the wet channels. During operation, the outdoor air (1) firstly passes through the dry channels of the IEC to get pre-cooled. Then the pre-cooled air (2) is directed to the evaporator to be further processed to the desired temperature and humidity. The room return air (4) is used as the working fluid in the wet channels, where it contacts with the sprayed water to induce the evaporative cooling effect. After leaving the wet channels, the room exhaust air (5) is directed to the condenser to remove a portion of the condensation heat. The remaining condensation heat is removed using the outdoor air (1') as the heat sink.



1

2 Figure 2 KAUST proprietary design of the IEC-MVC unit, states 1-7 refer to the locations in Figure 1

3

4 Figure 3 shows the photo of the pilot IEC-MVC unit. The unit is housed inside an aluminum frame. To
 5 minimize heat loss, the surfaces are covered with insulation materials. Three containers are put below the
 6 unit to collect the condensate produced in the evaporator and the dry channels, which is mixed with the
 7 external water source (RO water at a temperature of ~23 °C) and then supplied to the wet channels. The
 8 recovered condensate can reduce the water footprint of the process. Moreover, the condensate from the
 9 evaporator has the same temperature as the cold process air and will significantly promote the cooling
 10 performance of the IEC.

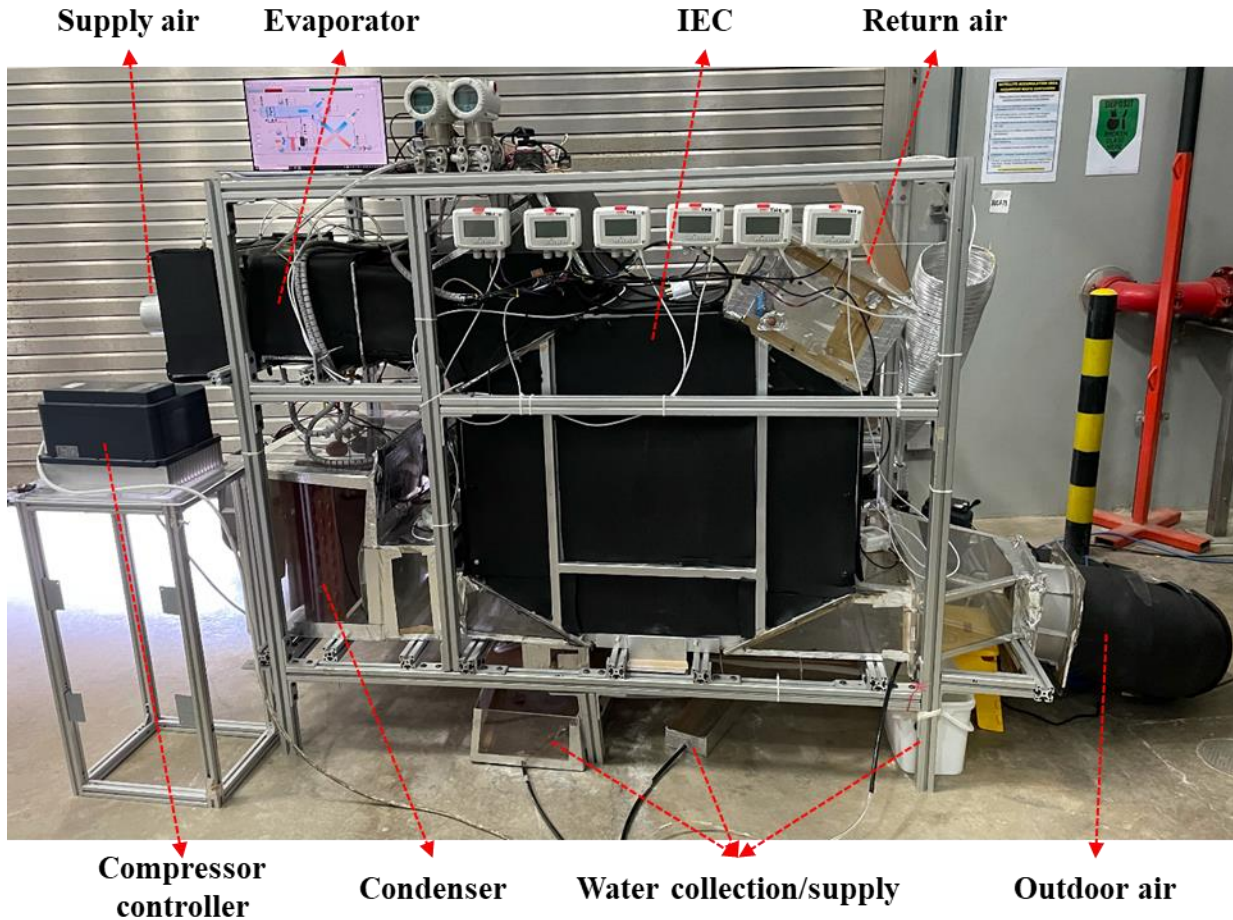


Figure 3 Pilot IEC-MVC unit at KAUST

During experimental tests, the room air is supplied to the wet channels, while a mixture of the outdoor air and the room air is supplied to the dry channels to control the temperature and humidity. A 2000 W hot-air gun is placed after the mixing chamber for further control of the inlet temperature. The flowrates of the air streams are regulated by changing the fan speed. Temperature and humidity sensors are installed at different locations (1-6) to monitor the air conditions, and flow nozzles and differential pressure gauges are installed at the exits of the dry and wet channels to measure the air flowrates. The power consumption of the compressor, the fans, and the spray pump are measured and recorded using digital power meters. The technical specifications of the sensors are summarized in Table 1.

Table 1 Technical data of measurement instrumentations

| Parameter | Sensor | Range | Accuracy |
|-------------------|--|----------|----------|
| Temperature | TJ36-44004-1/8-12, OMIGA | 0-60 °C | ±0.1 °C |
| Relative humidity | FH400, Degree Controls Inc. | 10-90% | ±2% |
| Pressure drop | 2600T Series Pressure Transmitter, ABB | 0-400 Pa | ± 5 Pa |
| Electrical power | PowerLogic PM5100, SCHNEIDER ELECTRIC | - | ±0.5% |

2.2 Performance indicators

Based on the measured parameters, the energy efficiency of the hybrid process, expressed as the coefficient of performance (COP), can be calculated. The COP is defined as the ratio of the cooling capacity to the energy input. For IEC, the COP is expressed as

$$COP_{IEC} = \frac{\dot{Q}_{IEC}}{P_{IEC}} = \frac{\dot{m}_{oa}(h_1 - h_2)}{P_{pump} + P_{fan,IEC}} \quad (1)$$

where \dot{Q}_{IEC} and P_{IEC} represent the cooling capacity and power consumption, respectively. \dot{m}_{oa} is the air flowrate in the dry channels, and h is the enthalpy of air. P_{pump} is the power consumption of the spray pump, and $P_{fan,IEC}$ is the overall electrical power of IEC fans.

Similarly, the COP of MVC and IEC-MVC can be calculated as

$$COP_{MVC} = \frac{\dot{Q}_{MVC}}{P_{MVC}} = \frac{\dot{m}_{oa}(h_2 - h_3)}{P_{comp} + P_{fan,IEC}} \quad (2)$$

$$COP_{IEC-MVC} = \frac{\dot{Q}_{total}}{P_{total}} = \frac{\dot{m}_{oa}(h_1 - h_3)}{P_{comp} + P_{pump} + P_{fan,IEC} + P_{fan,MVC}} \quad (3)$$

where P_{comp} is the compressor power, and $P_{fan,MVC}$ represents the power of the condenser fans.

In addition to the COP, the amount of cooling load handled by the IEC and the corresponding energy-saving are also important. The cooling capacity handled by IEC is computed as

$$\phi_{IEC} = \frac{\dot{Q}_{IEC}}{\dot{Q}_{total}} = \frac{\dot{m}_{oa}(h_1 - h_2)}{\dot{m}_{oa}(h_1 - h_3)} \quad (4)$$

And the energy-saving potential of the hybrid process over standalone MVC is derived as

$$\Delta COP = \frac{COP_{IEC-MVC} - COP_{MVC}}{COP_{IEC-MVC}} \quad (5)$$

One important difference between the proposed IEC-MVC process and standalone MVC (air-cooled) is that a certain amount of water is consumed in the IEC wet channels. Therefore, the amount of water consumption is also of great importance. The water consumption can be calculated from the change of moisture content in the wet channels

$$\dot{m}_{IEC} = \dot{m}_{ra}(\omega_5 - \omega_4) \quad (6)$$

Part of the water supply comes from the condensate collected from the supply air

$$\dot{m}_{cond} = \dot{m}_{oa}(\omega_1 - \omega_3) \quad (7)$$

Therefore, the net water consumption is expressed as

$$\dot{m}_{net} = \dot{m}_{IEC} - \dot{m}_{cond} \quad (8)$$

19

3. Results and discussion

This section presents the performance of the hybrid IEC-MVC process. The supply air conditions (temperature and humidity), energy efficiency, and water consumption are firstly evaluated under different conditions. Afterward, the energy-saving potential of the proposed IEC-MVC process over standalone MVC is discussed. Based on the derived results, a simplified model is developed for rapid prediction of IEC-MVC performance, and a case study is presented under the weather conditions of Saudi Arabia.

1

2 3.1 Cooling performance

3 The pilot IEC-MVC unit is tested under different outdoor air conditions (temperature, humidity ratio, and
4 flowrate) and compressor speeds. As the air supplied to the dry channels is a mixture of the outdoor air and
5 the room air, the temperature and humidity ratio are in the range of 30-40 °C and 10-20 g/kg, respectively.
6 The air flowrate in the dry channels is regulated between 250-460 CMH, and the wet channel air flowrate
7 is set to be close to the dry channel flowrate. This is because room exhaust air is used as the working air in
8 the wet channels, and the available amount is almost the same as the outdoor air intake. Finally, the
9 compressor frequency ranges 20-50 Hz. The parameter setting is summarized in Table 2.

10 Table 2 Parameter setting during experimental tests

| Parameter | Value/range |
|-----------------------------------|-------------|
| Outdoor air temperature (°C) | 30-40 |
| Outdoor air humidity ratio (g/kg) | 10-20 |
| Air flowrate (CMH) | 250-460 |
| Compressor frequency (Hz) | 20-50 |

11

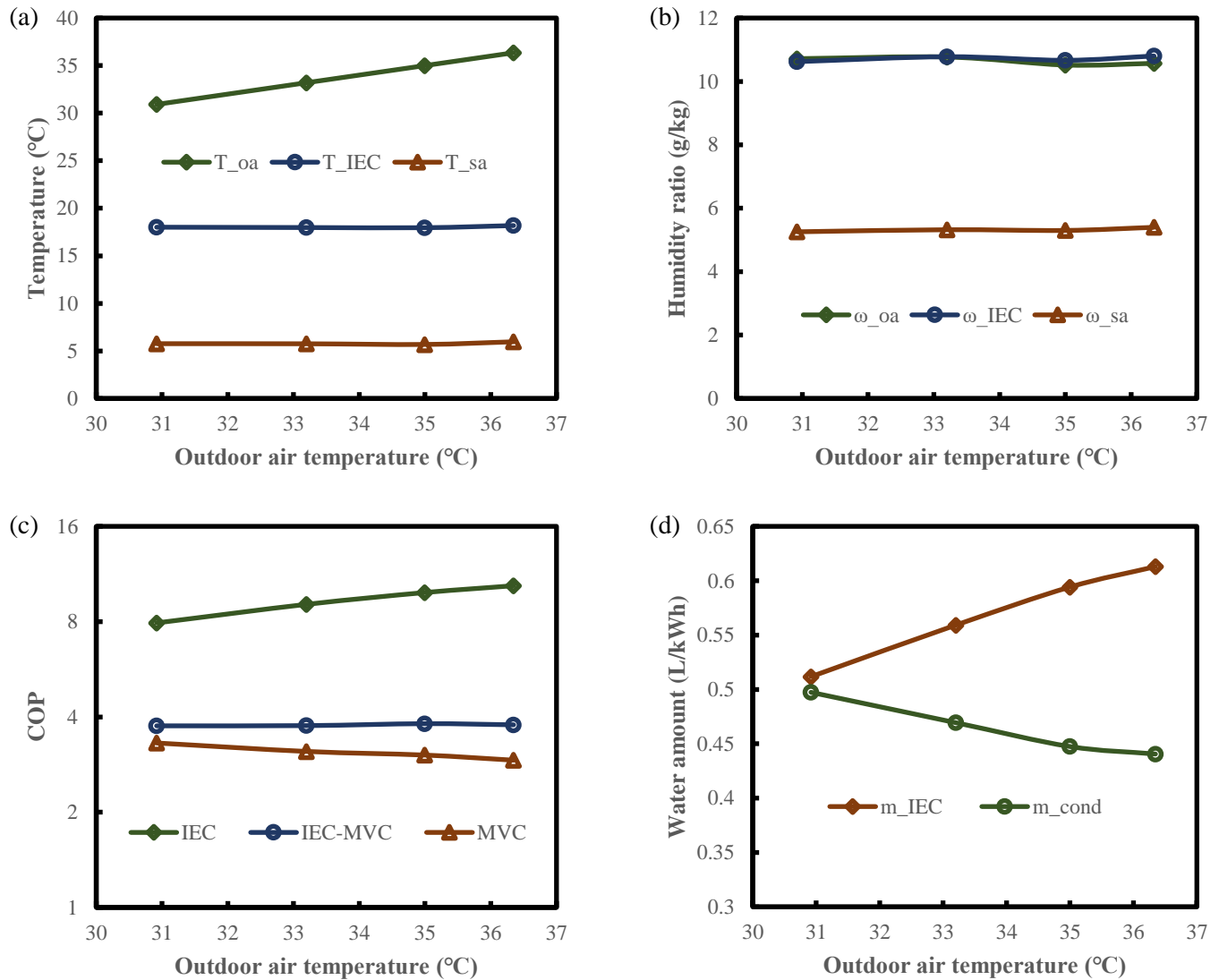
12 Figure 4 presents the system performance under different outdoor air temperatures with a fixed outdoor
13 humidity ratio of 10.6 g/kg. As shown in Figure 4(a), the IEC always cools the air to ~18 °C, regardless of
14 the outdoor air temperature. Such an observation differs from a regular IEC, whose outlet temperature
15 increases with the increase of inlet temperature [37]. The reason can be explained as follows. Firstly, the
16 working air flowrate in the wet channels of our system is close to that in the dry channels. This differs from
17 a regular IEC, where the wet channel flowrate is only 35-50% of the dry channel flowrate. A higher working
18 air flowrate induces more evaporative potential. Secondly, the cold condensate from the evaporator, which
19 has the same temperature as the off-coil air (~6 °C), is recovered and supplied to the wet channels to enhance
20 the cooling effect. Moreover, the outdoor air has low humidity and requires only sensible cooling. Therefore,
21 IEC is able to cool down the outdoor air to a similar temperature under different outdoor temperatures.
22 After the IEC, the evaporator coils further cool down the air to 6 °C.

23 Figure 4(b) shows the change in air humidity ratio. Similar to most IECs, the humidity ratio remains
24 constant along the dry channels, as the air temperature is higher than its dew point temperature. After
25 leaving the IEC, the air is dehumidified to 5 g/kg in the evaporator coils. The processed air (6 °C and 5
26 g/kg) can be mixed with the return air to achieve room thermal comfort.

27 Figure 4(c) plots the COP of IEC, MVC, and IEC-MVC under different outdoor air temperatures. With the
28 increase of the outdoor air temperature, the COP of IEC increases linearly due to more evaporative cooling
29 potential. On the other hand, the COP of MVC decreases with increasing outdoor air temperature, because
30 the compressor has to compress the refrigerant to a higher pressure for heat rejection. The conflicting effects
31 of temperature on IEC and MVC offset each other in the hybrid process, leading to little change in hybrid
32 COP.

33 The amounts of water consumption by IEC and condensate collection from the evaporator are plotted in
34 Figure 4(d). The values are normalized with respect to the total cooling capacity. As shown in the figure,
35 the water consumption in the wet channels is linearly proportional to the outdoor temperature, as the
36 evaporation of water is the main driving force for IEC cooling. On the other hand, the amount of condensate
37 per kWh of cooling capacity decreases with increasing temperature. This is because the net amount of water
38 collected remains the same (the evaporator always dehumidifies the outdoor air to 5 g/kg), while the cooling
39 capacity gets higher. The collected condensate can provide 72-95% of the water consumption in IEC, and
40 the need for external water supply is marginal at 0.01-0.17 L per kWh of cooling effect. The net water

- 1 consumption is much lower than that of a regular IEC (2-4 L/kWh under the weather condition of GCC
- 2 countries [8]), making the hybrid IEC-MVC applicable in arid areas that have limited access to fresh water.



3 Figure 4 Effect of outdoor air temperature on (a) outlet temperatures, (b) humidity ratio, (c) energy
 4 efficiency, and (d) water consumption. Outdoor humidity ratio = 10.6 g/kg, outdoor air flowrate = 300
 5 CMH, and compressor frequency = 20 Hz.

6

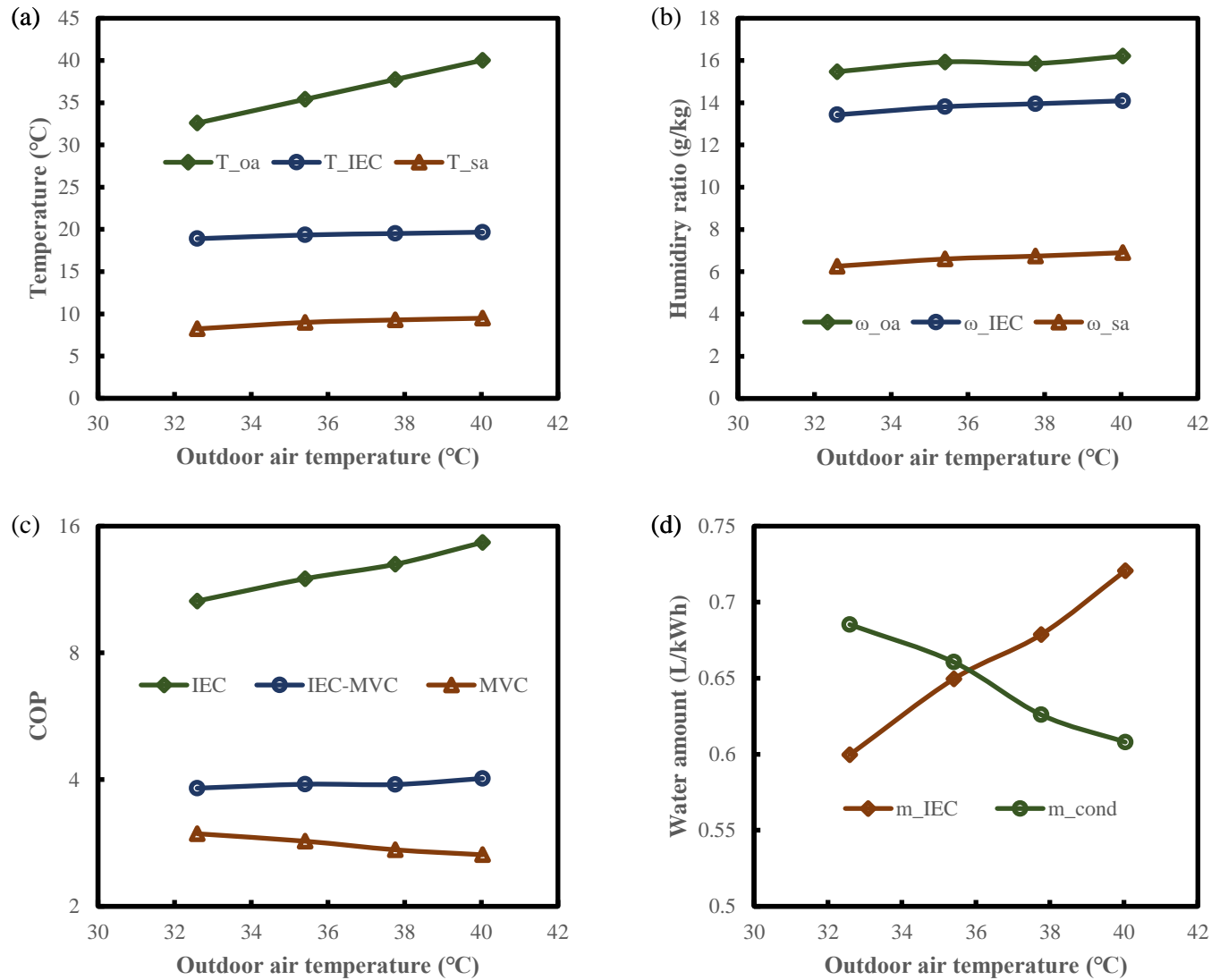
7 When the outdoor air humidity is high at 16 g/kg, the total cooling load increases, and the system shows a
 8 different response to temperature change. Compared with the low-humidity case, the air temperatures
 9 leaving IEC and MVC increase slightly with the increase in outdoor temperature, as revealed in Figure 5(a).
 10 Another major difference is that there is a drop in air humidity in the IEC, as shown in Figure 5(b). This is
 11 because the dew point temperature of the air is higher than the dry-bulb temperature in the dry channels.

12 Due to more drops of air enthalpy in the dry channels, the COP of IEC is higher at 10.5-14.5, as compared
 13 to 8-10 in the previous case. The overall trend of COP change remains the same, i.e., a higher outdoor

1 temperature promotes the COP of IEC while reducing the COP of MVC, and the hybrid COP remains
 2 constant.

3 With higher humidity, more condensate can be collected from the outdoor air, as can be seen in Figure 5(d).
 4 The condensation rate is 0.6-0.7 L/kWh in the present case, while the amount is lower at 0.4-0.5 L/kWh
 5 when the humidity ratio is 10.6 g/kg. The collected condensate is sufficient for the wet channels when the
 6 IEC cooling load is not too high, i.e., $T_{oa} < 36$ °C, and the excess condensate can be used somewhere else.

7



8 Figure 5 Effect of outdoor air temperature on (a) outlet temperatures, (b) humidity ratio, (c) energy
 9 efficiency, and (d) water consumption. Outdoor humidity ratio = 16 g/kg, outdoor air flowrate = 300
 10 CMH, and compressor frequency = 20 Hz.

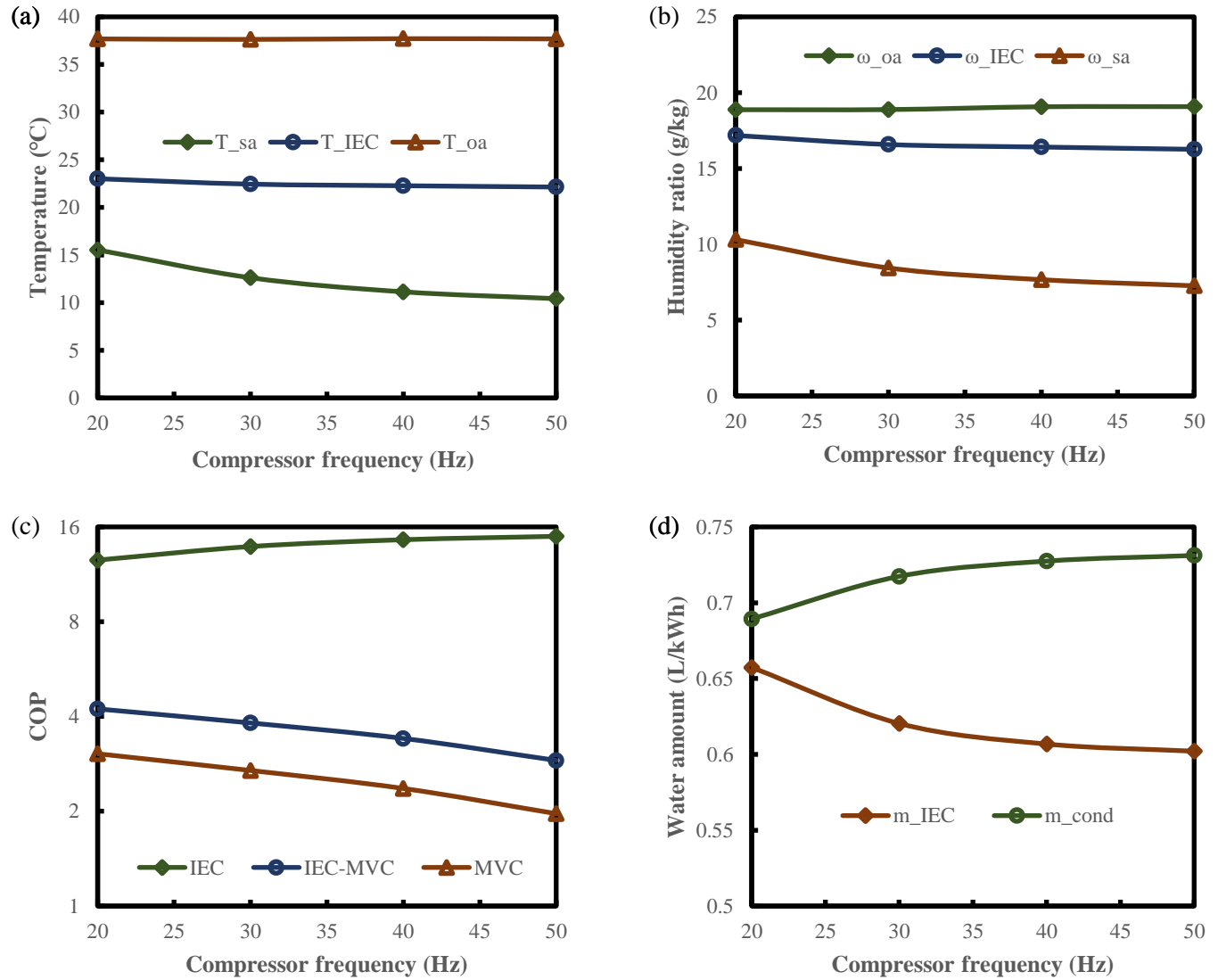
11

12 Figure 6 presents the system's response to the compressor frequency. With a higher compressor frequency,
 13 a lower evaporator temperature can be achieved. As a result, the air leaving the coils has a lower temperature
 14 and humidity, as can be seen in Figure 6(a) and Figure 6(b). The COP of MVC drops with compressor

1 frequency, as plotted in Figure 6(c). This is attributed to a higher compression ratio, which leads to more
 2 compression power. Finally, more condensate can be collected from the outdoor air due to a higher level of
 3 dehumidification, as shown in Figure 6(d).

4 The compressor frequency also has an impact on the performance of IEC. Under a higher compressor
 5 frequency, the condensate temperature is significantly reduced, as it follows the process air temperature.
 6 As a result, the performance of IEC is promoted. The air temperature and humidity are lower when leaving
 7 the IEC, leading to a higher COP. However, the hybrid COP shows a decreasing trend, as it is dominated
 8 by the MVC performance.

9



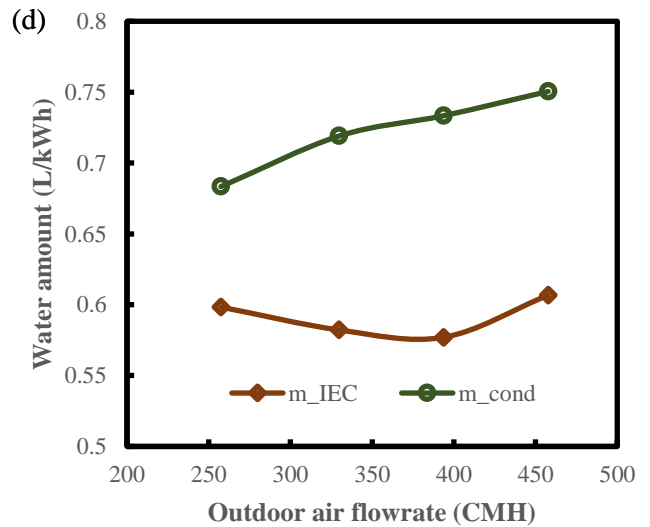
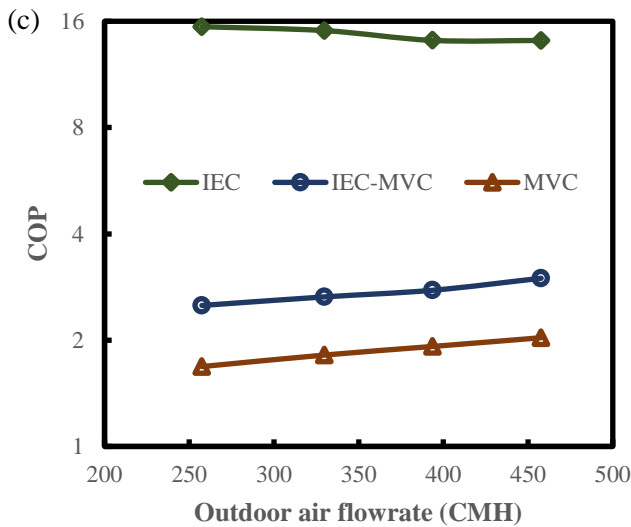
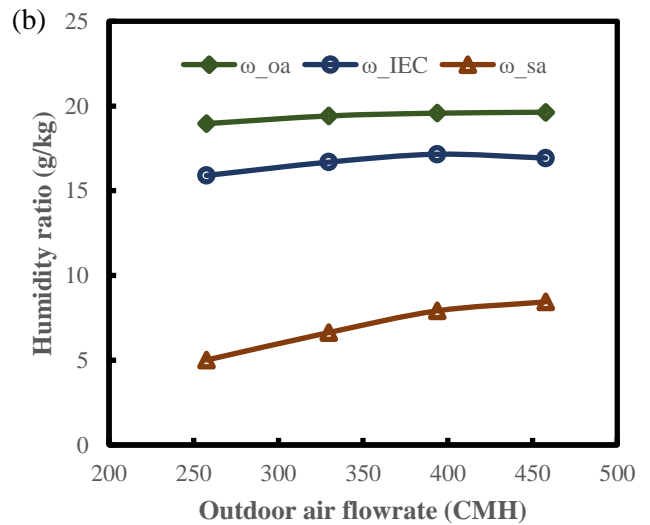
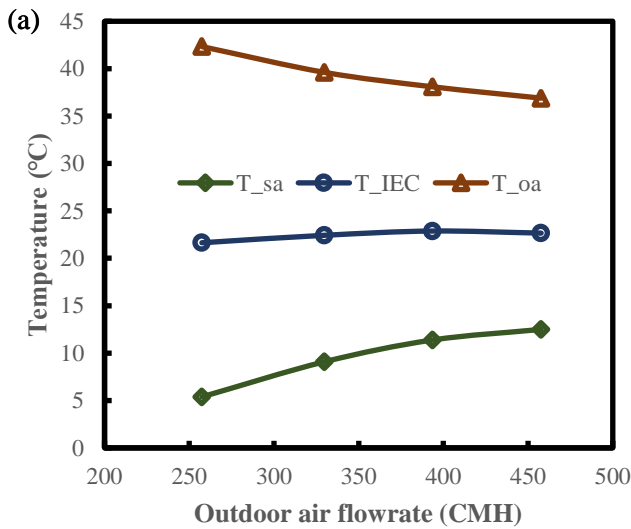
10 Figure 6 Effect of compressor frequency on (a) outlet temperatures, (b) humidity ratio, (c) energy
 11 efficiency, and (d) water consumption. Outdoor temperature = 38 °C, outdoor humidity ratio = 19 g/kg,
 12 and outdoor air flowrate = 350 CMH.

13

1 Figure 7 shows the system performance under different air flowrates. Due to a limited heater capacity, the
 2 inlet temperature drops with the flowrate. However, the air temperature and humidity are still higher when
 3 leaving the IEC (shown in Figure 7(a-b)), which is a result of a limited heat transfer area and a shorter
 4 contact time. For the same reason, the off-coil temperature and humidity ratio also increase with the flowrate,
 5 and the variations are more significant. Under the flowrate range considered, the supply air temperature and
 6 humidity ratio are varied by 7 °C and 3.5 g/kg, respectively. During practical operation, the flowrate can be
 7 an addition to the compressor frequency for controlling supply air condition and cooling load.

8 With a smaller temperature drop and a higher fan power, the COP of IEC drops with flowrate, as presented
 9 in Figure 7(c). However, the COP for MVC and the hybrid IEC-MVC process demonstrate a reverse trend,
 10 which is attributed to a higher evaporator temperature that lowers the compressor power. A higher air
 11 flowrate also introduces more moisture content into the system and leads to more condensation, as plotted
 12 in Figure 7(d). On the other hand, the water consumption of IEC firstly declines, and the trend is reversed
 13 after the flowrates exceed 400 CMH. The inflection point can be attributed to the increase of IEC cooling
 14 load, i.e. the drop of inlet temperature under a specific increment of air flowrate becomes less significant.

15



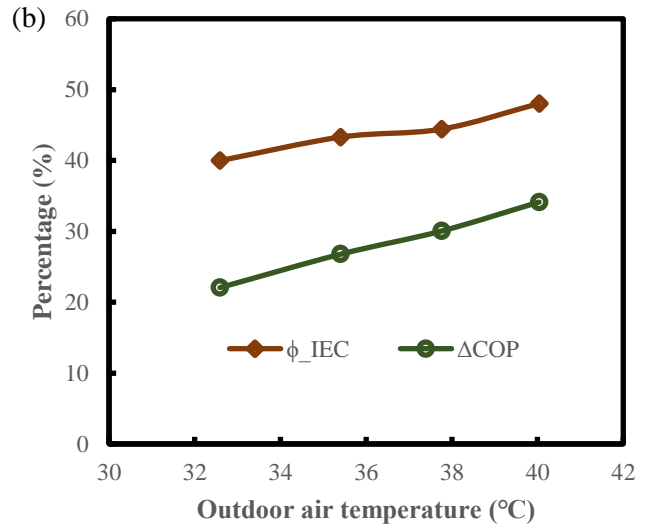
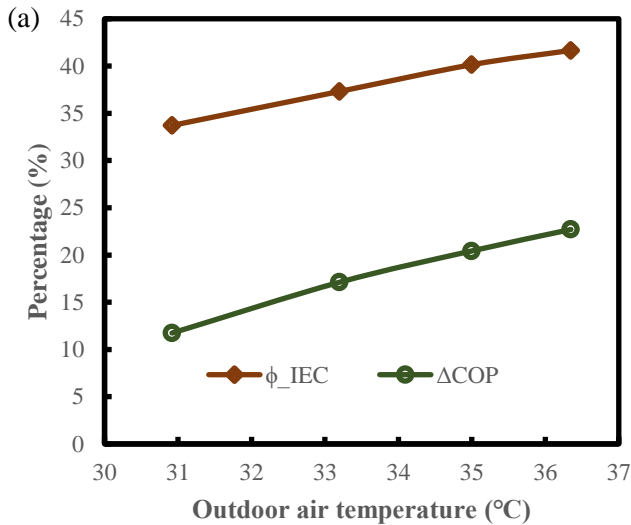
1 Figure 7 Effect of outdoor air flowrate on (a) outlet temperatures, (b) humidity ratio, (c) energy
 2 efficiency, and (d) water consumption. Outdoor temperature = 38 °C, outdoor humidity ratio = 19 g/kg,
 3 and compressor frequency = 50 Hz.

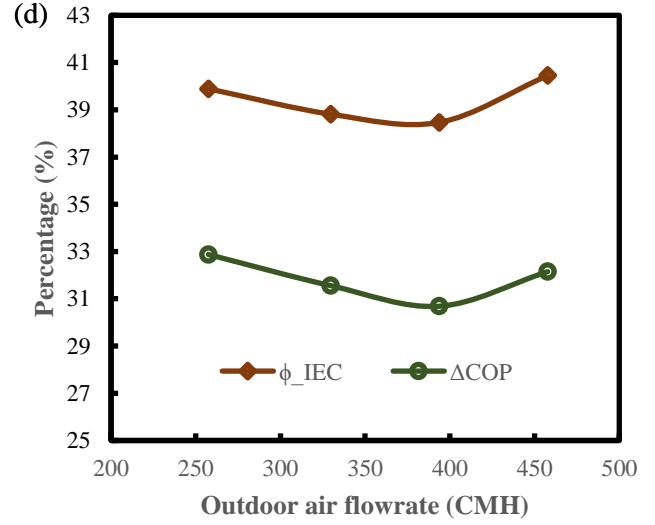
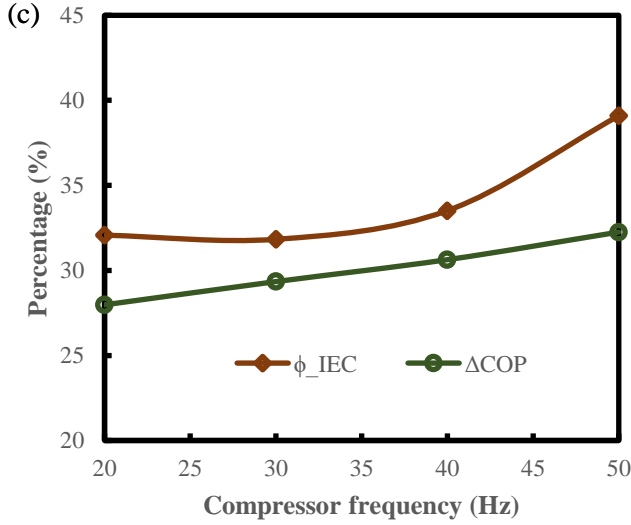
5 3.2 Energy saving potential

6 From the above results, it can be seen that the hybrid IEC-MVC process benefits from the high energy
 7 efficiency of IEC and has a higher COP than standalone MVC. The COP improvement is directly related
 8 to the percentage of cooling capacity contributed by IEC, as summarized in Figure 8. According to Figure
 9 8 (a-b), IEC handles a higher portion of cooling load when the outdoor temperature and humidity are higher,
 10 and the corresponding improvement of COP over MVC is also more obvious. Under a dry ambient
 11 condition, IEC handles up to 40% of the cooling load, and the hybrid COP is 22% higher than that of MVC.
 12 When the outdoor air is humid, the cooling capacity contributed by IEC can achieve 50%, leading to a 34%
 13 increase in COP.

14 A higher compressor speed also promotes IEC cooling capacity, which is caused by the supply of colder
 15 condensate to the wet channels. Consequently, the cooling capacity of IEC gets higher, and the
 16 improvement of COP is more significant, as shown in Figure 8 (c). When the compressor frequency
 17 increases from 20 to 50 Hz, the cooling load of IEC is increased from 32% to 39%, and the improvement
 18 of COP is varied from 28% to 32%.

19 Figure 8 (d) shows the COP improvement under different air flowrates. The numbers seem to be marginally
 20 impacted by the air flowrate. However, this is partially due to a reduced outdoor air temperature under a
 21 higher air flowrate, and it doesn't represent the intrinsic behavior of the system. If a constant outdoor air
 22 temperature is considered, more COP improvement can be expected under a higher air flowrate.





1 Figure 8 Energy-saving potential of IEC-MVC under different (a-b) outdoor air temperatures: (a) outdoor
 2 humidity ratio = 11 g/kg and (b) outdoor humidity ratio = 16 g/kg, (c) compressor frequency, and (d)
 3 outdoor air flowrate

4

5 3.3 Empirical model

6 Based on the derived results, we develop a simplified model that allows for a rapid evaluation of the IEC-
 7 MVC performance. The model firstly calculates the cooling capacity and energy efficiency of the IEC, then
 8 predicts the MVC performance, and finally analyzes the hybrid IEC-MVC process.

9 The cooling capacity of IEC can be calculated from the enthalpy effectiveness, which is defined as [28]

$$\varepsilon = \min \left\{ \frac{h_1 - h_2}{h_1 - h_{2,s}}, \frac{h_5 - h_4}{h_{5,s} - h_4} \right\} \quad (9)$$

10 where $h_{2,s}$ and $h_{5,s}$ represent the maximum/minimum enthalpy that the air streams can achieve, i.e., the
 11 outdoor air reaches the temperature of the room air when leaving the dry channels, and the room exhaust
 12 air in the wet channels has the same temperature as the incoming outdoor air.

13 According to our previous study, the effectiveness of IEC is determined by the temperature, humidity, and
 14 flowrate of the air streams [28]. The correlation is provided in Eq.10 and its discrepancy with the
 15 measurement is within 3.5%.

$$\varepsilon = 0.416 - 5.81 \times 10^{-3} T_{oa} + 4.65 \times 10^{-3} \omega_{oa} + 1.42 \times 10^{-3} T_{ra} - 5.65 \times 10^{-3} \omega_{ra} + 7.49 \times 10^{-4} \frac{\dot{m}_{oa}}{\dot{m}_{ra}} \quad (10)$$

16 Eq.9 and Eq.10 determine the change of air enthalpy in IEC, based on which the energy efficiency can be
 17 achieved. Figure 9 (a) shows the relationship between the enthalpy change and the COP. It is obvious that
 18 the COP of IEC is a linear function of the enthalpy change, which is expressed as

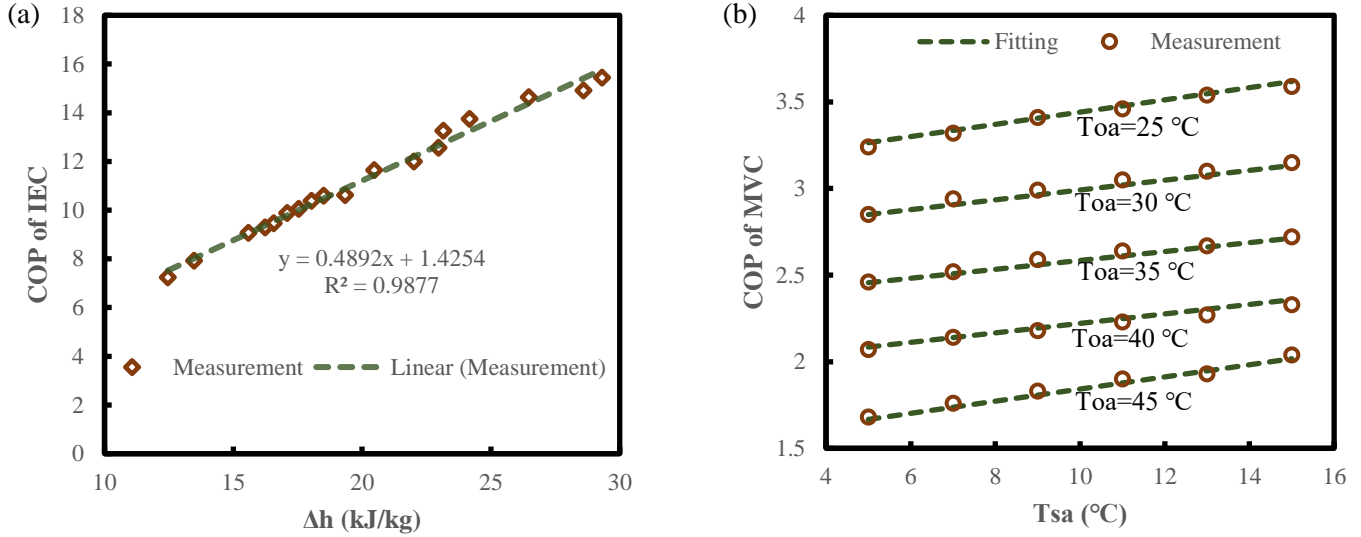
$$COP_{IEC} = 0.4892 \times \Delta h + 1.4254 \quad (11)$$

19 The coefficient of determination (R^2) is 0.9877, and the maximum deviation is 3.7%.

1 The energy efficiency of air-cooled MVC is determined by the temperature difference between the
 2 evaporator and the condenser, as plotted in Figure 9 (b). The relationship is quantified in Eq.12 with a
 3 maximum deviation of 3.1%.

$$COP_{MVC} = 0.0304 \times T_{sa} - 0.0761 \times T_{oa} + 4.992 \quad (12)$$

4



5 Figure 9 Comparison of measured COP with derived correlation for (a) IEC and (b) MVC

6

7 Employing the above equations, the performance of the IEC-MVC process can be easily estimated. Based
 8 on the temperature, humidity ratio, and flowrate of the outdoor air and room air, the cooling load, power
 9 consumption, and water consumption in the IEC can be calculated through Eqs.9-11 and Eq.6. Afterward,
 10 the supply air temperature and humidity can be determined by the total cooling load, based on which the
 11 energy consumption of MVC and the water footprint can be calculated using Eqs.7-8 and Eq.12. The
 12 process is schematically demonstrated in Figure 10. The proposed process is expected to have a high
 13 accuracy when the operating conditions are within our measurement range, i.e. outdoor air 30-42 °C and
 14 10-20 g/kg, room return air 23 ± 1 °C and 11 ± 1 g/kg, supply air temperature 5-15 °C (RH=100%) and
 15 return/outdoor air flowrate ratio 35-95%.

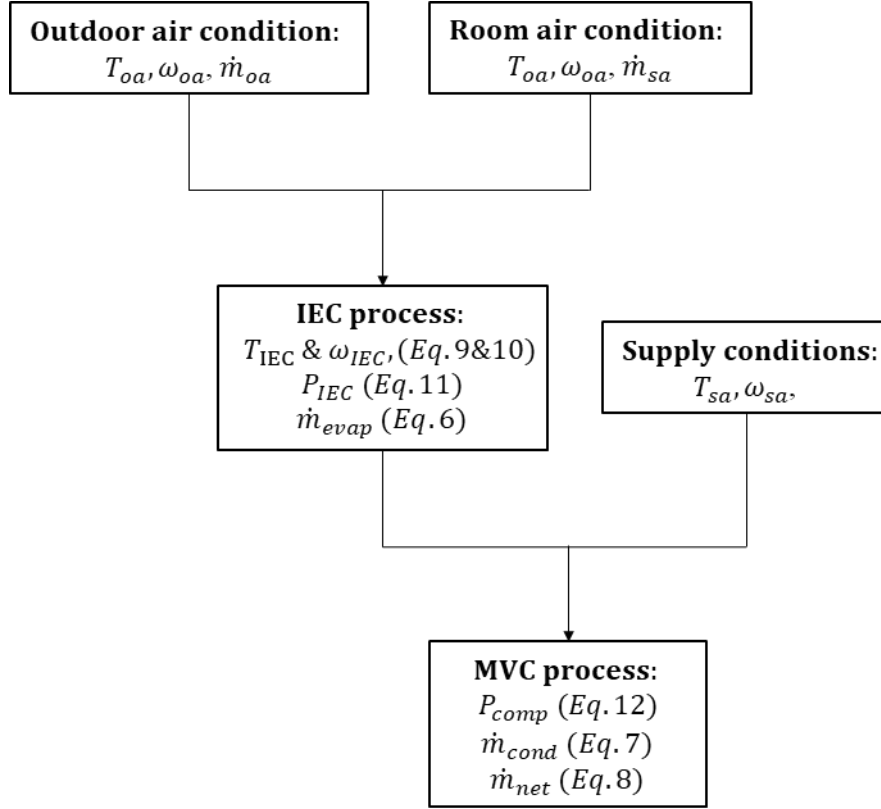


Figure 10 Rapid estimation of IEC-MVC performance

3.4 Case study in Saudi Arabia

Employing the simplified model, we estimate the annual energy-saving potential of IEC-MVC in the main cities of Saudi Arabia. 13 cities from different provinces are selected and their annual weather data (temperature and relative humidity) with an hourly resolution are acquired from Meteomatics Weather API [38]. To quantify the need for cooling and dehumidification, we introduce two parameters, namely, cooling degree hours (CDH) and dehumidifying gram hours (DGM). CDH is similar to the concept of cooling degree days (CDD) but calculated on an hourly basis:

$$CDH = \sum (T - 18^{\circ}\text{C}) \text{ when } T > 18^{\circ}\text{C} \quad (13)$$

where T is the hourly average temperature in $^{\circ}\text{C}$. CDH quantifies the amount of cooling demand and its duration. Similarly, DGM is a measurement of dehumidification demand in g/kg and its duration:

$$DGH = \sum (\omega - 9 \text{ g/kg}) \text{ when } \omega > 9 \text{ g/kg} \quad (14)$$

where ω is the hourly average humidity ratio of the ambient air.

The CDH and DGM for 13 representative cities of Saudi Arabia are summarized in the 4th and 5th columns of Table 3. Most cities have high cooling demand, as quantified by high values of CDH. Jazan has the maximum CDH of 111837 $^{\circ}\text{C}\cdot\text{hr}$, indicating an average cooling demand of 12.7 $^{\circ}\text{C}$ over the whole year (8760 hr). The CDH for Riyadh, Qassim, Dhahran, Makkah and Madinah also exceed 80000 $^{\circ}\text{C}\cdot\text{hr}$. Abha and Al-Bahah, in contrast, have little cooling demand due to a high latitude of $> 2000 \text{ m}$. In addition to the sensible cooling demand, certain cities also need dehumidification due to high ambient humidity. These

1 cities include Dhahran (DGH=22225 g-hr/kg), Makkah (DGH=22225 g-hr/kg) and Jazan (DGH=58262 g-
2 hr/kg).

3 Columns 6-7 in Table 3 show the contributions of IEC and the energy-saving over standalone MVC. The
4 proposed system shows excellent performance in hot and dry cities, i.e. Riyadh, Hail, Qassim, Al-Jouf,
5 Turaif, Tabuk, Madinah and Najran. In these cities, IEC can handle >50% of the total cooling load, leading
6 to 40-60% of energy savings. In hot and humid cities (Dhahran, Mecca and Jazan), the performance
7 degrades slightly, but there is still ~20% of energy saving.

8 The last two columns summarize the water footprint. The water consumption of IEC is in the range of 6-20
9 L/hr for 1 kg/s of outdoor air, depending on the cooling load of IEC. Such water consumption can be
10 compensated by the condensate collected in the MVC evaporator. For example, the collected condensate
11 can account for 46% and 58% of the water consumption in Makkah and Dhahran, respectively. In Jazan,
12 the amount of condensate is more than the water consumption, and the excess water can be used elsewhere.

13 Table 3 Long-term performance of IEC-MVC in different cities of Saudi Arabia

| Region | Province | Representative city | CDH, °C-hr/year | DGH, g-hr/year | $\phi_{IEC}, \%$ | Energy saving, % | Water consumption, L/hr | Water collection, L/hr |
|--------|------------------|---------------------|-----------------|----------------|------------------|------------------|-------------------------|------------------------|
| Middle | Ar-Riyadh | Riyadh | 92248.4 | 432.57 | 54.35 | 40.52 | 8.57 | 0.18 |
| | Hail | Hail | 71265.4 | 6.84 | 53.65 | 37.57 | 6.33 | 0.00 |
| | Al-Qassim | Qassim | 88722.4 | 124.65 | 54.96 | 40.98 | 8.21 | 0.04 |
| East | Eastern Region | Dhahran | 89967.1 | 22225.80 | 31.27 | 26.04 | 9.15 | 8.25 |
| | Al-Jouf | Al-Jouf | 65980.4 | 9.24 | 53.71 | 37.83 | 5.87 | 0.00 |
| | Northern Borders | Turaif | 48481.6 | 86.82 | 50.14 | 33.44 | 3.94 | 0.01 |
| West | Tabuk | Tabuk | 62562.6 | 155.29 | 51.94 | 36.12 | 5.36 | 0.03 |
| | Makkah | Mecca | 107079.7 | 21044.16 | 32.77 | 24.78 | 10.86 | 7.90 |
| | Al-Madinah | Madinah | 101092.6 | 995.84 | 53.49 | 40.15 | 9.53 | 0.25 |
| South | Aseer | Abha | 17674.9 | 815.62 | 15.32 | 7.55 | 0.38 | 0.01 |
| | Jazan | Jazan | 111837.0 | 58262.63 | 22.39 | 17.20 | 12.22 | 23.56 |
| | Najran | Najran | 58329.4 | 409.75 | 45.09 | 28.13 | 4.29 | 0.11 |
| | Al-Bahah | Al-Bahah | 20167.7 | 1113.43 | 15.46 | 7.87 | 0.51 | 0.04 |

14

15 4. Conclusions

16 A pilot IEC-MVC unit is fabricated and tested under different conditions to evaluate its performance,
17 including the capability of temperature and humidity control, the energy-saving potential over MVC, and
18 the water footprint. The following concluding remarks can be derived from the results:

- 1 (1) The IEC can pre-cool the outdoor air to ~ 20 °C by recovering cold energy from the room exhaust
 2 air. When the outdoor humidity is high, IEC also dehumidifies the outdoor air by 1-2 g/kg;
 3 (2) The pre-cooled air can be further processed to 5-15 °C and 5-10 g/kg by MVC. The supply air
 4 temperature and humidity can be regulated by changing the compressor frequency and the air
 5 flowrate;
 6 (3) The IEC handles 35-50% of the total cooling load, and the energy consumption of the hybrid
 7 process is 15-35% lower than standalone MVC;
 8 (4) The recovered condensate can compensate for >70% of water consumption in IEC. When the
 9 outdoor humidity is high, the system produces excess freshwater;
 10 (5) The proposed process is suitable for most cities in Saudi Arabia. The energy-saving potential of the
 11 system is higher in hot and dry regions, while the water footprint is smaller in humid areas.

12

13 **Nomenclature**

Abbreviations

| | |
|------------|------------------------------|
| <i>AC</i> | Air conditioning |
| <i>CDD</i> | Cooling degree days |
| <i>CDH</i> | Cooling degree hours |
| <i>COP</i> | Coefficient of performance |
| <i>DGH</i> | Dehumidifying gram hours |
| <i>IEC</i> | Indirect evaporative cooler |
| <i>MVC</i> | Mechanical vapor compression |

Symbols

| | |
|----------|----------------------------|
| <i>h</i> | Specific enthalpy, J/kg |
| <i>m</i> | Mass flowrate, kg/s |
| <i>P</i> | Electricity consumption, W |
| <i>Q</i> | Cooling load, W |
| <i>T</i> | Temperature, °C |
| <i>X</i> | Cooling load ratio, % |

Greek letters

| | |
|---------------|--|
| ε | Effectiveness, % |
| ϕ | Percentage of cooling load handled by IEC, % |
| ω | Humidity ratio, g/kg |

Subscripts

| | |
|-------------|-----------------------|
| <i>comp</i> | Compressor |
| <i>cond</i> | Condensation |
| <i>evap</i> | Evaporation |
| <i>fan</i> | Fan |
| <i>ma</i> | Mixed air |
| <i>net</i> | Net water consumption |
| <i>oa</i> | Outdoor air |
| <i>pump</i> | Pump |

| | |
|--------------|------------------|
| <i>ra</i> | Room exhaust air |
| <i>s</i> | Saturated |
| <i>sa</i> | Supply air |
| <i>total</i> | Total |

1

2 Acknowledgement

3 This research was supported by the Water Desalination and Reuse Center (WDRC), King Abdullah
4 University of Science and Technology (KAUST).

5

6 References

- 7 [1] IEA, *Global air conditioner stock, 1990-2050*, . IEA, Paris [https://www.iea.org/data-and-](https://www.iea.org/data-and-statistics/charts/global-air-conditioner-stock-1990-2050)
8 [statistics/charts/global-air-conditioner-stock-1990-2050](https://www.iea.org/data-and-statistics/charts/global-air-conditioner-stock-1990-2050), 2021.
- 9 [2] Evely, V. and D.S. Ayou, *Sustainable district cooling systems: Status, challenges, and future*
10 *opportunities, with emphasis on cooling-dominated regions*. *Energies*, 2019. **12**(2): p. 235.
- 11 [3] Shahzad, M.W., M. Burhan, D. Ybyraimkul, S.J. Oh, and K.C. Ng, *An improved indirect*
12 *evaporative cooler experimental investigation*. *Applied Energy*, 2019. **256**: p. 113934.
- 13 [4] Shahzad, M.W., J. Lin, B.B. Xu, L. Dala, Q. Chen, M. Burhan, M. Sultan, W. Worek, and K.C. Ng,
14 *A spatiotemporal indirect evaporative cooler enabled by transiently interceding water mist*. *Energy*,
15 2021. **217**: p. 119352.
- 16 [5] Jradi, M. and S. Riffat, *Experimental and numerical investigation of a dew-point cooling system*
17 *for thermal comfort in buildings*. *Applied Energy*, 2014. **132**: p. 524-535.
- 18 [6] Min, Y., Y. Chen, and H. Yang, *Numerical study on indirect evaporative coolers considering*
19 *condensation: A thorough comparison between cross flow and counter flow*. *International Journal*
20 *of Heat and Mass Transfer*, 2019. **131**: p. 472-486.
- 21 [7] Yang, H., W. Shi, Y. Chen, and Y. Min, *Research development of indirect evaporative cooling*
22 *technology: An updated review*. *Renewable and Sustainable Energy Reviews*, 2021. **145**: p. 111082.
- 23 [8] Baakeem, S.S., J. Orfi, A. Mohamad, and S. Bawazeer, *The possibility of using a novel dew point*
24 *air cooling system (M-Cycle) for A/C application in Arab Gulf Countries*. *Building and*
25 *Environment*, 2019. **148**: p. 185-197.
- 26 [9] Oh, S.J., M.W. Shahzad, M. Burhan, W. Chun, C.K. Jon, M. KumJa, and K.C. Ng, *Approaches to*
27 *energy efficiency in air conditioning: a comparative study on purge configurations for indirect*
28 *evaporative cooling*. *Energy*, 2019. **168**: p. 505-515.
- 29 [10] Cui, X., M. Islam, and K. Chua, *An experimental and analytical study of a hybrid air-conditioning*
30 *system in buildings residing in tropics*. *Energy and Buildings*, 2019. **201**: p. 216-226.
- 31 [11] Duan, Z., C. Zhan, X. Zhao, and X. Dong, *Experimental study of a counter-flow regenerative*
32 *evaporative cooler*. *Building and Environment*, 2016. **104**: p. 47-58.
- 33 [12] Jia, L., J. Liu, C. Wang, X. Cao, and Z. Zhang, *Study of the thermal performance of a novel dew*
34 *point evaporative cooler*. *Applied Thermal Engineering*, 2019. **160**: p. 114069.
- 35 [13] Pandelidis, D., E. Niemierka, A. Pacak, P. Jadwiszczak, A. Cichoń, P. Drag, W. Worek, and S.
36 Cetin, *Performance study of a novel dew point evaporative cooler in the climate of central Europe*
37 *using building simulation tools*. *Building and Environment*, 2020. **181**: p. 107101.
- 38 [14] Wang, F., T. Sun, X. Huang, Y. Chen, and H. Yang, *Experimental research on a novel porous*
39 *ceramic tube type indirect evaporative cooler*. *Applied Thermal Engineering*, 2017. **125**: p. 1191-
40 1199.
- 41 [15] Duan, Z., C. Zhan, X. Zhang, M. Mustafa, X. Zhao, B. Alimohammadisagvand, and A. Hasan,
42 *Indirect evaporative cooling: Past, present and future potentials*. *Renewable and Sustainable*
43 *Energy Reviews*, 2012. **16**(9): p. 6823-6850.

- 1 [16] Boukhanouf, R., O. Amer, H. Ibrahim, and J. Calautit, *Design and performance analysis of a*
2 *regenerative evaporative cooler for cooling of buildings in arid climates*. Building and
3 Environment, 2018. **142**: p. 1-10.
- 4 [17] Riffat, S. and J. Zhu, *Mathematical model of indirect evaporative cooler using porous ceramic and*
5 *heat pipe*. Applied Thermal Engineering, 2004. **24**(4): p. 457-470.
- 6 [18] Park, J.-Y., B.-J. Kim, S.-Y. Yoon, Y.-S. Byon, and J.-W. Jeong, *Experimental analysis of*
7 *dehumidification performance of an evaporative cooling-assisted internally cooled liquid desiccant*
8 *dehumidifier*. Applied Energy, 2019. **235**: p. 177-185.
- 9 [19] Moshari, S. and G. Heidarinejad, *Analytical estimation of pressure drop in indirect evaporative*
10 *coolers for power reduction*. Energy and Buildings, 2017. **150**: p. 149-162.
- 11 [20] Kabeel, A., M. Bassuoni, and M. Abdelgaied, *Experimental study of a novel integrated system of*
12 *indirect evaporative cooler with internal baffles and evaporative condenser*. Energy Conversion
13 and Management, 2017. **138**: p. 518-525.
- 14 [21] Kabeel, A. and M. Abdelgaied, *Numerical and experimental investigation of a novel configuration*
15 *of indirect evaporative cooler with internal baffles*. Energy conversion and management, 2016. **126**:
16 p. 526-536.
- 17 [22] Ali, M., W. Ahmad, N.A. Sheikh, H. Ali, R. Kousar, and T. ur Rashid, *Performance enhancement*
18 *of a cross flow dew point indirect evaporative cooler with circular finned channel geometry*.
19 Journal of Building Engineering, 2021. **35**: p. 101980.
- 20 [23] Zhao, X., S. Liu, and S.B. Riffat, *Comparative study of heat and mass exchanging materials for*
21 *indirect evaporative cooling systems*. Building and Environment, 2008. **43**(11): p. 1902-1911.
- 22 [24] Rashidi, S., M.H. Kashefi, K.C. Kim, and O. Samimi-Abianeh, *Potentials of porous materials for*
23 *energy management in heat exchangers—A comprehensive review*. Applied energy, 2019. **243**: p.
24 206-232.
- 25 [25] Boukhanouf, R., A. Alharbi, H.G. Ibrahim, O. Amer, and M. Worall, *Computer modelling and*
26 *experimental investigation of building integrated sub-wet bulb temperature evaporative cooling*
27 *system*. Applied Thermal Engineering, 2017. **115**: p. 201-211.
- 28 [26] Lee, J. and D.-Y. Lee, *Experimental study of a counter flow regenerative evaporative cooler with*
29 *finned channels*. International Journal of Heat and Mass Transfer, 2013. **65**: p. 173-179.
- 30 [27] Chen, Y., H. Yang, and Y. Luo, *Indirect evaporative cooler considering condensation from*
31 *primary air: Model development and parameter analysis*. Building and Environment, 2016. **95**: p.
32 330-345.
- 33 [28] Chen, Q., M.K. Ja, M. Burhan, F.H. Akhtar, M.W. Shahzad, D. Ybyraiymkul, and K.C. Ng, *A*
34 *hybrid indirect evaporative cooling-mechanical vapor compression process for energy-efficient air*
35 *conditioning*. Energy Conversion and Management, 2021. **248**: p. 114798.
- 36 [29] Cui, X., K. Chua, M. Islam, and K.C. Ng, *Performance evaluation of an indirect pre-cooling*
37 *evaporative heat exchanger operating in hot and humid climate*. Energy Conversion and
38 Management, 2015. **102**: p. 140-150.
- 39 [30] Duan, Z., X. Zhao, J. Liu, and Q. Zhang, *Dynamic simulation of a hybrid dew point evaporative*
40 *cooler and vapour compression refrigerated system for a building using EnergyPlus*. Journal of
41 Building Engineering, 2019. **21**: p. 287-301.
- 42 [31] Chen, Y., Y. Luo, and H. Yang, *Fresh air pre-cooling and energy recovery by using indirect*
43 *evaporative cooling in hot and humid region—a case study in Hong Kong*. Energy procedia, 2014.
44 **61**: p. 126-130.
- 45 [32] Cui, X., L. Sun, S. Zhang, and L. Jin, *On the study of a hybrid indirect evaporative pre-cooling*
46 *system for various climates*. Energies, 2019. **12**(23): p. 4419.
- 47 [33] Chen, Y., H. Yang, and Y. Luo, *Parameter sensitivity analysis and configuration optimization of*
48 *indirect evaporative cooler (IEC) considering condensation*. Applied energy, 2017. **194**: p. 440-
49 453.

- 1 [34] Chen, Y., Y. Luo, and H. Yang, *A simplified analytical model for indirect evaporative cooling*
2 *considering condensation from fresh air: Development and application*. Energy and Buildings,
3 2015. **108**: p. 387-400.
- 4 [35] Pandelidis, D., A. Cichoń, A. Pacak, S. Anisimov, and P. Drag, *Counter-flow indirect evaporative*
5 *cooler for heat recovery in the temperate climate*. Energy, 2018. **165**: p. 877-894.
- 6 [36] Min, Y., Y. Chen, and H. Yang, *A statistical modeling approach on the performance prediction of*
7 *indirect evaporative cooling energy recovery systems*. Applied Energy, 2019. **255**: p. 113832.
- 8 [37] Chen, Q., M. Burhan, M.W. Shahzad, D. Ybyraiymkul, F.H. Akhtar, and K.C. Ng, *Simultaneous*
9 *production of cooling and freshwater by an integrated indirect evaporative cooling and*
10 *humidification-dehumidification desalination cycle*. Energy Conversion and Management, 2020.
11 **221**: p. 113169.
- 12 [38] <https://www.meteomatics.com/en/weather-api/>.

13